

Hemodynamics of Focal Versus Global Growth of Small Cerebral Aneurysms

Paolo Machi¹ · Rafik Ouared¹ · Olivier Brina¹ · Pierre Bouillot^{1,2} · Hasan Yilmaz¹ · Maria I Vargas¹ · Renato Gondar³ · Philippe Bijlenga³ · Karl O Lovblad¹ · Zsolt Kulcsár^{1,4}

Received: 6 July 2017 / Accepted: 12 October 2017
© Springer-Verlag GmbH Germany 2017

Abstract

Background and Purpose Hemodynamics play a driving role in the life cycle of brain aneurysms from initiation through growth until eventual rupture. The specific factors behind aneurysm growth, especially in small aneurysms, are not well elucidated. The goal of this study was to differentiate focal versus general growth and to analyze the hemodynamic microenvironment at the sites of enlargement in small cerebral aneurysms.

Materials and Methods Small aneurysms showing growth during follow-up were identified from our prospective aneurysm database. Three dimensional rotational angiography (3DRA) studies before and after morphology changes were available for all aneurysms included in the study, allowing for detailed shape and computational fluid dynamic (CFD) based hemodynamic analysis. Six patients fulfilled the inclusion criteria.

Results Two different types of change were observed: focal growth, with bleb or blister formation in three, and global

aneurysm enlargement accompanied by neck broadening in other three patients. Areas of focal growth showed low shear conditions with increased oscillations at the site of growth (a low wall shear stress [WSS] and high oscillatory shear index [OSI]). Global aneurysm enlargement was associated with increased WSS coupled with a high spatial wall shear stress gradient (WSSG).

Conclusion For different aneurysm growth types, distinctive hemodynamic microenvironment may be responsible and temporal–spatial changes of the pathologic WSS would have the inciting effect. We suggest the distinction of focal and global growth types in future hemodynamic and histological studies.

Keywords Cerebral aneurysm · Aneurysm growth · Subarachnoid hemorrhage · Computational flow · Dynamics

Abbreviations

3D	Three-dimensional
ICA	Internal carotid artery
MRA	Magnetic resonance angiography
CTA	Computed tomographic angiography
3DRA	Three-dimensional rotational angiography
WSS	Wall shear stress
WSSG	Wall shear stress gradient
OSI	Oscillatory shear index
GA	Growth area (of the aneurysm wall)
LVF	Low value fraction
HVF	High value fraction
DSA	Digital subtraction angiography
STL	STereoLithography

Electronic supplementary material The online version of this article (<https://doi.org/10.1007/s00062-017-0640-6>) contains supplementary material, which is available to authorized users.

✉ Zsolt Kulcsár
kulcsarzsolt22@gmail.com

¹ Neuroradiology Division, Department of Radiology and Medical Informatics, Geneva University Hospitals, Geneva, Switzerland

² Laboratory for Hydraulic Machines, École Polytechnique Fédérale de Lausanne, Lausanne, Switzerland

³ Neurosurgery Division, Department of Clinical Neurosciences, Geneva University Hospitals, Geneva, Switzerland

⁴ Department of Neuroradiology, University Hospital of Zurich, Frauenklinikstraße 10, 8091 Zürich, Switzerland

Introduction

The number of incidentally detected unruptured aneurysms is continuously increasing due to the broader availability of noninvasive brain imaging; thus, specialists are faced more often with the crucial question of whether an aneurysm should be preventively treated. Although general risk factors are usually widely considered, aneurysm size, shape, and location remain the most important decisive factors [1–3]. The number of followed patients with small untreated aneurysms is increasing, which makes it possible to observe these small lesions over the longer term and allow for observation of growth.

The frequency of growing aneurysms is estimated to be approximately 3% per year [4]. Although the risk factors for growth are similar to the risk factors for rupture, the exact mechanisms and the process of aneurysm growth are not well understood and sometimes controversial. The role of hemodynamic factors in initiating biological processes in the vessel wall, both in atherosclerotic and aneurysmal disease, is being increasingly recognized; however, the specific hemodynamic mechanisms behind the biological processes of structural wall changes are still not well elucidated and apparently quite controversial. The most important hemodynamic factor considered to play a leading role in changing the pathophysiology of the vessel wall and aneurysm wall is wall shear stress (WSS). WSS is the tangential, frictional force of the flowing viscous blood on the endothelial lining. Abnormally high or low WSS will induce different pathological changes of the vessel wall. So far both high and low WSS have been implicated in changing aneurysm wall structure, growth and rupture status, leading to quite some confusion. It is important to note however that WSS is not a *constant force* but one which *shows temporal and spatial changes* through the cardiac cycle. It has been shown that the spatial and temporal alternation of WSS throughout the cardiac cycle may induce morphological changes of the vessel wall resembling aneurysm initiation [5, 6]; however, its role in the eventual growth of *already developed aneurysms* has not yet been addressed. Our goal in this study was to assess this concept in patients with small aneurysms demonstrating growth during follow-up.

Material and Methods

Patients

This study is based on the prospective database of aneurysm patients recruited in the @neurIST project, approved by the local ethics committee. Baseline characteristics were collected for all recruited patients, including patient his-

tory, risk factors for intracranial aneurysms development and rupture, as well as number of aneurysms, location and morphological description. The subgroup of patients with unruptured aneurysms and conservative management (regular follow-up protocol) was considered for analysis, as previously described [7]. From this group all patients harboring small unruptured aneurysms with size or morphology change (growing aneurysms) during the follow-up have been selected. The criteria for growth were met as previously described, i. e., ≥ 1 mm in one dimension or ≥ 0.5 mm in at least 2 dimensions, or indisputable shape change, with development of a bleb [8]. For further analysis we included only those unstable aneurysms that underwent a catheter angiography study with 3DRA reconstruction of the target lesion at the initial (aneurysm detection) time point. This was necessary to allow for high resolution 3D dataset based high definition segmentation. Growing aneurysms with only CTA or MRA studies, but no catheter angiogram based 3DRA reconstruction were thus excluded from further analysis, to avoid spatial resolution-related bias. The growth was detected as follows: (1) incidentally found by the regular follow-up visits, (2) diagnosed by patients reporting unusual headaches or other symptoms, (3) visualized due to aneurysm rupture. After the suspicion of growth was raised by CTA or MRA, it was confirmed by regular DSA with 3DRA. The baseline and follow-up DSA and 3DRA datasets were compared allowing for objective assessment of change in size and morphology. The type of change was defined as *focal* if only a small region of the aneurysm wall (less than 15%) had undergone changes without affecting the neck size, leading to “bleb”, “blister” or “daughter-aneurysm” like deformation. *Global* growth was considered if a larger area of the aneurysm wall has enlarged accompanied by important aneurysm neck broadening.

Imaging Work-up and CFD Analysis

The 3DRA DICOM datasets were obtained from the reconstruction on Philips Healthcare TM Xtravision, of 50–75% of angioscoped vessel tree, and were stacked in 256^3 pixel reconstruction matrix. Then, in-house automatic watershed-based segmentation provided the 3D-rendered virtual images of the aneurysms in their specific artery environments in STL format. Two geometry models (pre- and post-growing) were provided for each patient, in total, 12 models. Each geometry model was used, on one side, for assessment of geometry factors, and on the other side, for flow modeling.

As to the geometry factors, aneurysm size, surface, volume, neck size, neck surface, apex (the one-dimensional height of the aneurysm from the center of the neck to the dome) and aspect ratio were considered in

the analysis. The careful examination by an experienced operator of pre- (initial time point) and post-growth differences between the three-dimensional (3D) aneurysm image datasets has allowed identifying the sites of aneurysm growing.

The geometry properties related to aneurysm growing were analyzed beforehand, independently of any hemodynamic properties. Second, hemodynamic properties and how they may couple to geometry factors were addressed. The STL models were meshed in ANSYS ICEMCFD (ANSYS Inc., Canonsburg, PA, USA, v14.5) with patch-dependent method for shell, and robust-octree method for volume tetra/mixed dominant mesh type, along with three boundary layers of prism. Voxel resolutions were fixed at 0.2 mm and 0.1 mm in artery and aneurysm domains, respectively. The typical number of mesh elements oscillated between 3.5 and 5.7 million, whereas density of the latter ranged between 3000 and 4500 elements/mm³. The 3D incompressible Navier–Stokes equations were solved with ANSYS-CFX solver for pulsatile flow simulations. The inlet flow boundary conditions were all applied to ICA inlets based on Womersley velocity profile and generic one-dimensional flow standard waveforms [9]. Typical mean flow rates were either 4.36cc/s (right ICA) or 3.94 cc/s (left ICA). The differences in outlet pressures were around 200 Pa, for mean dynamic pressures ranging between 3300 and 3600 Pa. ICA inlet mass flow rates were scaled with the specific inlet area (diameter varies between 3.6 and 5.1 mm) and vessel walls were assumed rigid, while blood was approximated as a Newtonian fluid with a density of 1060 kg/m³ and a dynamic viscosity of 3.5 cP. For each cycle 100 time-steps were considered [10]. The instantaneous velocity, absolute wall shear stress (WSS) and absolute wall shear stress spatial gradient (WSSG) fields computed in the second cardiac

cycle were saved for offline analysis, along with the oscillating shear stress index (OSI).

For every time step of the cardiac cycle, both WSS and WSSG fields in the aneurysm domain were extracted from ANSYS-CFX result file, along with one oscillating shear stress index (OSI). We first checked whether significant scaling trend on space-averaged velocity, WSS and WSSG cardiac cycle profiles may occur in first and second control aneurysms, and in/off the overall growing sites, too.

Then, we focused on the initial (before growth) morphology to analyze the differences in OSI, WSS, and WSSG patterns that might be responsible for the growth. The patterns were representing the spatial dispersion of OSI and peak systolic values of WSS and WSSG, respectively.

To analyze quantitatively the figures, we first identified the growth areas (GA) in the initial morphology with a semi-automatic clusterization methodology, and then compared the density distribution functions of OSI, peak systolic WSSG and WSS in GA and the whole aneurysm. Three parameters were used: (1) spatial means (\pm standard deviation, SD), (2) median values, and (3) the average fractions of OSI, WSSG and WSS values in growth areas, below median (low value fraction, LVF, %) and above median (high value fraction, HVF, %), respectively (Eq. 1). If HVF is larger than 1.5 times LVF, the type of shear was flagged as “HIGH”, otherwise it was “LOW” in the inverse proportion, or neither high nor low in the last case.

$$\begin{aligned}
 LVF_i &= \frac{1}{x_i^{\text{median}}} \int_0^{x_i^{\text{median}}} \frac{f_{\{ga\}}(x_i)}{g_{\{an\}}(x_i)} dx_i, HVF_i \\
 &= \frac{1}{(x_i^{\text{max}} - x_i^{\text{median}})} \int_{x_i^{\text{median}}}^{x_i^{\text{max}}} \frac{f_{\{ga\}}(x_i)}{g_{\{an\}}(x_i)} dx_i
 \end{aligned}
 \tag{1}$$

Table 1 Summary of patient and aneurysm characteristics

Patients	Age	Gender	Aneurysm location	Initial size (mm)	Risk factors	Time (months) between aneurysm detection and sign of growth	Aneurysm volume increase (%)	Neck enlargement (%)	Type of growth	Accompanying symptoms
P1	61	M	L MCA	1.7	None	73	216	20	Global	None
P2	43	M	R A1 segment	4.0	None	27	11	11	Focal	None
P3	69	M	ACoMA	2.9	HT	60	87	39	Global	None
P4	44	M	L ICA bifurcation	2.8	Smoking, substance abuse, former SAH	103	1086	190	Global	SAH
P5	46	F	R PComA	2.3	HT, smoking	38	61	19	Focal	Alarming headaches
P6	44	F	R AChorAnt	2.7	None	54	116	1	Focal	Alarming headaches

M male, F female, L left, R right, ICA internal carotid artery, ACoMA anterior communicating artery, PComA posterior communicating artery, AChorAnt anterior choroidal artery, MCA middle cerebral artery, SAH subarachnoid hemorrhage

where x_i refers to OSI, WSSG or WSS variables, x_i^{\max} and x_i^{median} are the maximum and median values of x_i ; $f_{i_{ga}}(x_i)$ and $g_{i_{an}}(x_i)$ are the density distribution functions of variables in the growth area and whole aneurysm, respectively. Histograms of the density functions are showed in Figs. 3 and 4 for “focal” and “global” groups, respectively (see Supplementary Electronic Material).

Results

Altogether six patients fulfilled the selection criteria. Their mean age at the discovery of the six unruptured aneurysms was 51 years and four were male. The initial aneurysm size ranged between 1.5 and 4.0 mm. General risk factors are listed in Table 1. The mean time to growth detection was 59 ± 30 months. One aneurysm had ruptured, 2 patients

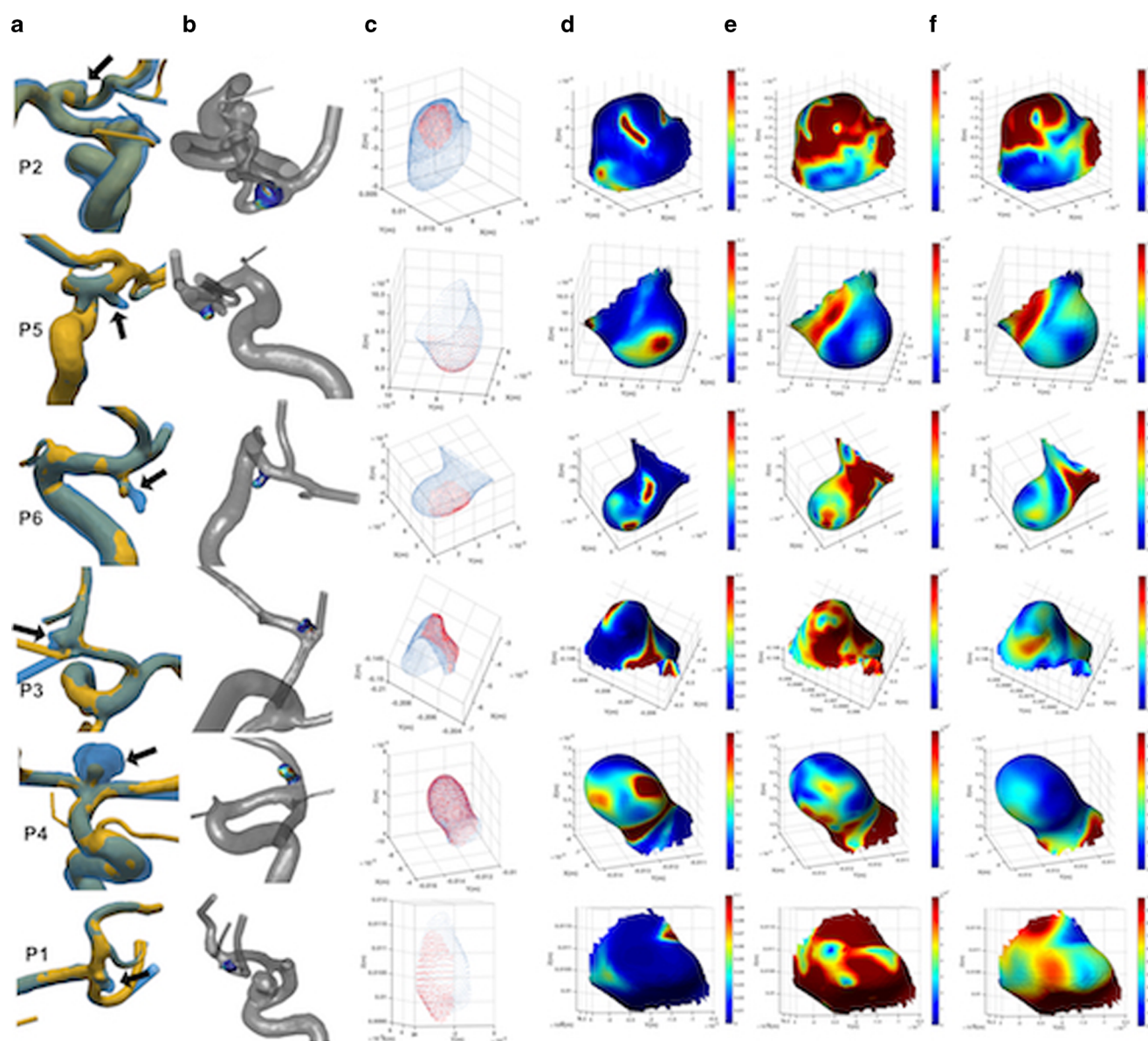
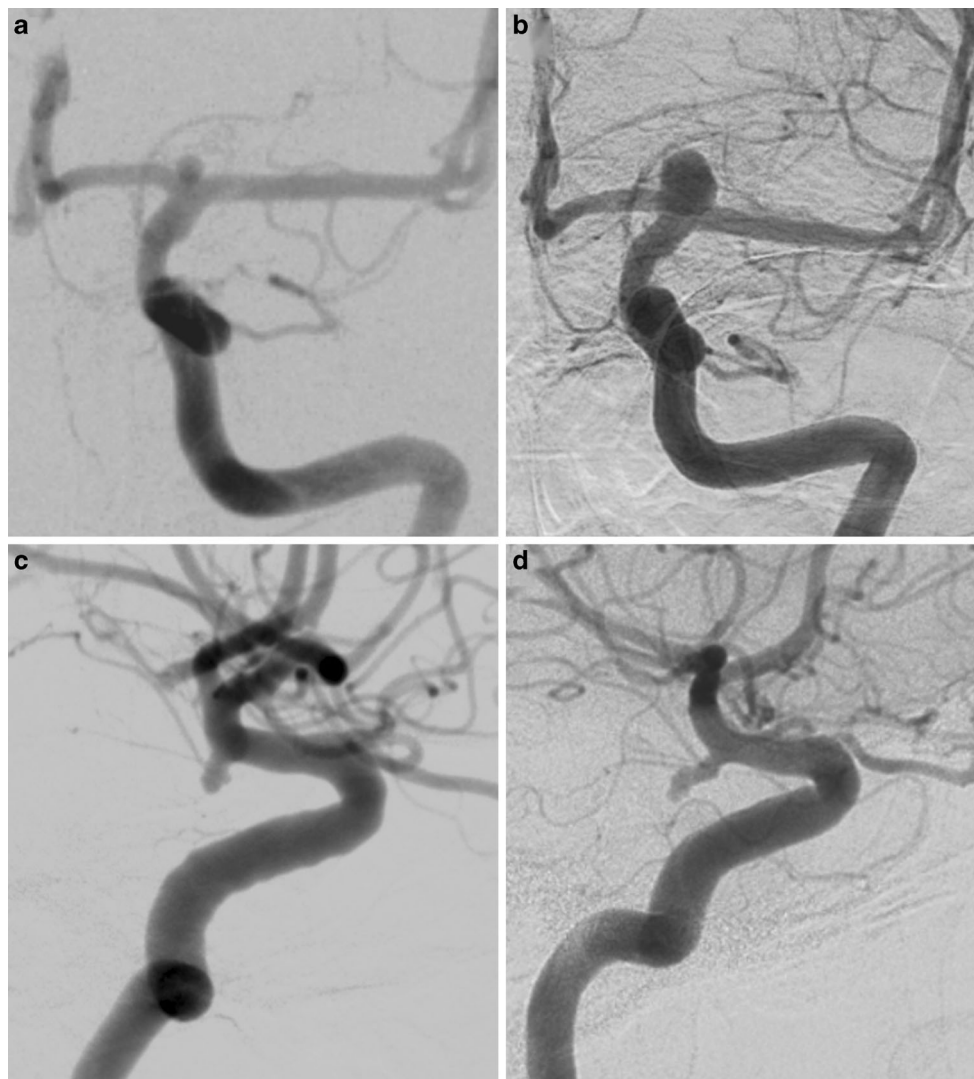


Fig. 1 Aneurysm growth representations: Every patient is represented in a given row by 6 columns ranging from **a–f**. The first 3 rows (P2, P5, P6) and last 3 rows (P3, P4, P1) undergo “focal” and “diffuse” growth, respectively. The fusion of arterial segments at first detection of aneurysms (yellow) and at follow-up (blue) is represented in **a**. The projection views in **a**, have been chosen to better highlight for each aneurysm, where and how aneurysms growth occurred **b**. The projection views in **b–f** are different from those in **a**, for each aneurysm (row), respectively: they are meant to highlight the specific flow pattern features in the so-called “hemodynamic projection view”. **d–f** show the oscillatory shear index (OSI) and systolic wall shear stress gradient (WSSG) and wall shear stress (WSS), respectively. The red cloud points in **c** show the growth areas in detected aneurysms (blue cloud points): in the first three rows, the growth areas are focalized in small regions, while in the last three, the growth areas are more diffuse. **b** contextualizes, within the same “hemodynamic projection view”, the aneurysms in their vessel environments. The aneurysms are represented with their OSI patterns, respectively

Fig. 2 Examples of two different growth types. Digital subtraction angiography (DSA) of a patient (P4) with a small, unruptured internal carotid artery (ICA) terminus aneurysm, showing a global enlargement and rupture after a period of 103 months (**a,b**). Unruptured aneurysm of the anterior choroidal artery showing focal growth (bleb formation) accompanied by severe headaches 49 months after initial detection (**c,d**)



presented unusual headaches during the follow-up that led to emergency imaging and in 3 patients the growth was clinically silent and detected upon regular follow-up visits. All aneurysms were treated as rupture or growth was detected. Regarding the type of growth, three aneurysms (P2, P5, P6) developed *focal deformation* (bleb/blister formation) and three aneurysms (P1, P3, P4) showed *global enlargement* accompanied by neck increase.

Growth-Related Hemodynamics

The aneurysms showing focal growth (bleb/blister formation) demonstrated a typical hemodynamic microenvironment specific to the site where the morphology change took place. This was marked by high oscillatory flow and low focal WSS. The WSSG and the WSS around the spot of high OSI was not specific, being either high or moderate (Fig. 1d for P2, P5 and P6). For the aneurysms with general growth the coupling of prominent positive WSSG and

WSS values especially affected the neck area and more dispersed parts of the aneurysm dome where the enlargement took place, without relevant OSI figures, although the average OSI values in the GA were higher than in the whole aneurysm (Fig. 1e and f, P3, P4 and P1). These aneurysms have shown neck enlargement and increase in size without bleb formation. Detailed quantified analysis is in the online supplement (Suppl. Figures 1, 2 and 3 and Suppl. Table).

Discussion

In this longitudinal follow-up of small unruptured aneurysms two different growth types were identified and analyzed from the hemodynamic aspect, respectively the *focal* aneurysm shape change with bleb/blister formation, and the *general* aneurysm growing coupled with neck enlargement (Fig. 2). For the two growth types, two different hemodynamic microenvironments were found to play a decisive

Table 2 List of articles classified based on the type of growth and growth related hemodynamic parameters

Article	No. of cases studied	Hemodynamic parameters			Flow pattern	Comments
		WSS	WSSG	OSI		
<i>Focal growth</i>						
Cebral et al. 2010 [19]	20AA/30 blebs	High (80%), low (20%)	NT	NT	Bleb aligned to inflow/outflow jet	Digital bleb removal
Shojima et al. 2010 [20]	4	Low	High	Not studied	Not studied	Real bleb
Tanoue et al. 2011 [21]	1	Low	High	Not studied	Recirculation at the site of bleb formation	Real bleb
Sugiyama et al. 2012 [22]	1	High	Not studied	Low	Not studied	Real bleb
Russel et al. 2013 [23]	27	High	–	Not related	Bleb aligned to inflow/outflow jet	Digital bleb removal
Sugiyama et al. 2016 [24]	1	High	Not studied	Not studied	Bleb aligned to inflow/outflow jet	Real bleb
<i>Global growth</i>						
Bousel et al. 2008 [25]	7	Low	Not studied	Not studied	Not studied	Growth type not specified
Sugiyama et al. 2012 [22]	1	Low	Not studied	High	Not studied	Real enlargement
Brinjikji et al. 2016 [26]	12	Low	Not studied	Low	Vorticity	Growth type not specified
Sforza et al. 2016 [27]	16	Non-uniform WSS	Not studied	High	Complex, with nonuniform WSS	Growth type not specified; from 16 growing only 6 aneurysms with growth >1 mm

AA aneurysms, WSS wall shear stress, WSSG wall shear stress gradient, OSI oscillatory shear index

role. For bleb formation high focal OSI values coupled with low WSS were consecutively found. For neck enlargement accompanied general aneurysm growth high WSS coupled with elevated positive WSSG was presumed to be responsible, affecting the neck and larger areas of the aneurysm dome.

Growth is usually detected by longitudinal imaging follow-up of patients harboring unruptured cerebral aneurysms. According to recent data approximately 3–6% of all aneurysms will grow each year [4, 11, 12], small aneurysms being affected in 2.6–4.5% [4, 7, 12]. The medical risk factors recognized for growth are quite similar to the well-known risk factors for aneurysm rupture: older age, smoking, female sex, irregular shape, size at detection and posterior circulation [4, 7, 11–13]. The risk of rupture of aneurysms with detected growth is more difficult to assess, since growing aneurysms are in general considered unstable and are treated. According to some estimations, growth will increase the risk of rupture by a factor of ten [14, 15]. The annual rate of rupture after growth is 3.1% [4], but numbers vary between 2.4% [15] and 18.5% [14]. Unfortunately, the risk of rupture associated with different types of growth, i. e., bleb formation versus global enlarge-

ment, have not yet been clearly addressed in the literature and data are lacking if the rupture risk would be different.

Understanding the biological mechanisms behind aneurysm growth is as important as understanding mechanisms leading to aneurysm initiation and rupture. It has been generally accepted that local hemodynamic forces will drive biological reactions in the vessel or aneurysm wall. Hypothesizing that a similar mechanism may be responsible for all three events in the life cycle of aneurysms (initiation, growth and stabilization or rupture) may be logical; however, literature data are not very well aligned in this regard. For aneurysm initiation high WSS conditions are held responsible [5, 6, 16, 17]. Once an aneurysm has been formed, the hemodynamic conditions responsible for growth or rupture are thought to change as well [18] and several findings from different research groups have proposed different mechanisms for growth and eventual rupture. This resulted in apparently confounding mass of data challenging high versus low flow theories, conflicting the *low flow related, inflammatory reaction driven* versus the *high flow related, mural cell driven wall degeneration* (Table 2).

Growth is a prerequisite in the life cycle of an aneurysm, since without the phase of growing an aneurysm will not develop. It has been suggested that growth occurs in irreg-

ular and discontinuous phases rather than constantly [28]. Having in mind that all aneurysms need to grow (otherwise they could not be detected), it becomes evident that only some of them will bleed despite the common thought that growth seems to be an independent risk for rupture. The majority of aneurysms will thus remain stable over long periods of time.

There are only a few hemodynamic flow studies dealing with the hemodynamic microenvironment preceding shape change and unfortunately also even fewer distinguishing between the hemodynamics of bleb formation and global enlargement (Table 2). The methodologies of hemodynamic assessment of bleb formation and the results are not consistent in the literature. Nevertheless, in the majority of cases published, where rather high flow conditions were implicated in the blister formation, digital bleb removal was used to analyze the hemodynamics before growth [19, 23]. This technique is used due to the fact that only a small number of aneurysms are detected with real bleb formation during follow-up, with sufficient quality imaging of the initial status to allow for CFD simulations. Although seemingly very pragmatic, this approach may predispose to significant errors due to the fact that a lobulation or bleb on the aneurysm sac does not necessarily mean that this bleb formed at a second time-point, but it may have already been present at the very beginning, at the primary formation of the aneurysm. In such a case, speculations on predisposing hemodynamic microenvironment may be out of scope.

Impinging flow or high flow and high WSS adjacent of bleb/blister formation was detected in studies with artificial bleb removal or post-bleb formation [19, 23, 24, 29]. In studies with real pre-bleb status simulation [20–22], the low WSS areas were identified, in agreement with our findings.

In the literature low WSS was also hold responsible for growth in general, without specifying the type of growth (global or focal) and the hemodynamic microenvironment at the site of growth [22, 25–27]. For the global enlargement we focused our analysis on the well-defined areas where enlargement took place and found similar results to studies where elevated WSS coupled with elevated WSSG was found responsible for mural cell mediated wall remodeling [5, 6, 30, 31]. This kind of growth mechanism is similar to what is found in the initiation phase of an aneurysm life cycle and would clearly explain the enlargement of the aneurysm sac accompanied by the enlargement of the neck/orifice area.

A recently published human series of hemodynamics coupled with a histological analysis of affected aneurysm walls has demonstrated that aneurysm wall inflammation was associated with high, low and heterogeneous WSS with endothelial damage and luminal thrombus formation. In contrary, aneurysm wall degeneration with loss of mural cells was detected in aneurysms with low flow conditions;

however, inflammation was also detected in degenerated walls [32]. The findings of this study correlate with our findings of hemodynamic microenvironment necessary for bleb formation.

The contradictions in the current literature related to intra-aneurysmal hemodynamic-related wall changes may be related to the lack of specification of the type of growth that took place. We know that altered WSS is present in the whole vascular tree and will affect the endothelial cells. According to our current hypothesis and understanding, to achieve destructive remodeling this affection needs to be catalyzed by the temporal and spatial alterations of the WSS during a cardiac cycle (like high gradients and oscillations of WSS).

Limitations

The major limitation of the study is the low number of subjects which prevents us to generalize the observation. The low number is explained by the exigency we posed towards high definition segmentation, which is important in small aneurysms. This high definition segmentation can currently be based only on 3DRA, which will further exclude patients from the study, since currently the majority of patients with small aneurysms will not encounter DSA during their follow-up.

Geometry and hemodynamic modeling may induce bias on end results that are difficult to assess. Limitations are mainly due to complexity of anatomy or to lack of specificity of generic flow properties. Magnitudes of hemodynamic factors should be considered with appropriate care and caution, since generic boundary conditions were used; however, in the analysis the relative values were considered important.

Conclusion

In the phase of growth cerebral aneurysms may show different types of changes with either global growth with enlargement of the aneurysm dome together with the orifice or focal changes on the aneurysm dome with bleb or blister formation. This paper demonstrated that these two growth types need to be separated for hemodynamic analysis, since the mechanisms may be different: for global growth with neck enlargement rather high flow conditions with increased WSS coupled with positive WSSG were observed at the areas of enlargement (neck and dome), similar to the hemodynamics of aneurysm initiation. Bleb formation was associated with rather low WSS with high OSI. This work underlined again that not necessarily the magnitude, but the temporo-spatial changes of the WSS would have the inciting effect. We recommend the clear differentiation of

different growth types in future hemodynamic and histology studies.

Funding This study was supported by Swiss National Science Foundation grants (SNF 32003B_160222 and SNF 320030_156813).

Conflict of interest P. Machi, R. Ouared, O. Brina, P. Bouillot, H. Yilmaz, M.I. Vargas, R. Gondar, P. Bijlenga, K.O. Lovblad and Z. Kulcsár declare that they have no competing interests.

References

- Morita A, Kirino T, Hashi K, Aoki N, Fukuhara S, Hashimoto N, Nakayama T, Sakai M, Teramoto A, Tominari S, Yoshimoto T. The natural course of unruptured cerebral aneurysms in a Japanese cohort. *N Engl J Med*. 2012;366:2474–82.
- Wiebers DO, Whisnant JP, Huston J 3rd, Meissner I, Brown RD Jr, Piegras DG, Forbes GS, Thielen K, Nichols D, O'Fallon WM, Peacock J, Jaeger L, Kassell NF, Kongable-Beckman GL, Torner JC; International Study of Unruptured Intracranial Aneurysms Investigators. Unruptured intracranial aneurysms: natural history, clinical outcome, and risks of surgical and endovascular treatment. *Lancet*. 2003;362:103–10.
- Greving JP, Wermer MJH, Brown RD, Morita A, Juvela S, Yonekura M, Ishibashi T, Torner JC, Nakayama T, Rinkel GJE, Algra A. Development of the PHASES score for prediction of risk of rupture of intracranial aneurysms: a pooled analysis of six prospective cohort studies. *Lancet Neurol*. 2014;13:59–66.
- Brinjikji W, Zhu YQ, Lanzino G, Cloft HJ, Murad MH, Wang Z, Kallmes DF. Risk factors for growth of intracranial aneurysms: a systematic review and meta-analysis. *AJNR Am J Neuroradiol*. 2016;37:615–20.
- Meng H, Wang Z, Hoi Y, Gao L, Metaxa E, Swartz DD, Kolega J. Complex hemodynamics at the apex of an arterial bifurcation induces vascular remodeling resembling cerebral aneurysm initiation. *Stroke*. 2007;38:1924–31.
- Metaxa E, Tremmel M, Natarajan SK, Xiang J, Paluch RA, Mandelbaum M, Siddiqui AH, Kolega J, Mocco J, Meng H. Characterization of critical hemodynamics contributing to aneurysmal remodeling at the basilar terminus in a rabbit model. *Stroke*. 2010;41:1774–82.
- Gondar R, Gautschi OP, Cuony J, Perren F, Jägersberg M, Corniola MV, Schatlo B, Molligaj G, Morel S, Kulcsár Z, Mendes Pereira V, Rüfenacht D, Schaller K, Bijlenga P. Unruptured intracranial aneurysm follow-up and treatment after morphological change is safe: observational study and systematic review. *J Neurol Neurosurg Psychiatr*. 2016;87:1277–82.
- Backes D, Vergouwen MD, Tiel Groenestege AT, Bor AS, Velthuis BK, Greving JP, Algra A, Wermer MJ, van Walderveen MA, terBrugge KG, Agid R, Rinkel GJ. PHASES score for prediction of intracranial aneurysm growth. *Stroke*. 2015;46:1221–6.
- Reymond P, Merenda F, Perren F, Rüfenacht D, Stergiopoulos N. Validation of a one-dimensional model of the systemic arterial tree. *Am J Physiol Heart Circ Physiol*. 2009;297:H208–H22.
- Pereira VM, Brina O, Gonzales MA, Narata AP, Bijlenga P, Schaller K, Lovblad KO, Ouared R. Evaluation of the influence of inlet boundary conditions on computational fluid dynamics for intracranial aneurysms: a virtual experiment. *J Biomech*. 2013;46:1531–9.
- Backes D, Rinkel GJ, Laban KG, Algra A, Vergouwen MD. Patient- and aneurysm-specific risk factors for intracranial aneurysm growth: a systematic review and meta-analysis. *Stroke*. 2016;47:951–7.
- Bor AS, Groenestege TT, terBrugge KG, Agid R, Velthuis BK, Rinkel GJ, Wermer MJ. Clinical, radiological, and flow-related risk factors for growth of untreated. *Stroke*. 2015;46:42–8.
- Burns JD, Huston J, Layton KF, Piegras DG, Brown RD. Intracranial aneurysm enlargement on serial magnetic resonance angiography: frequency and risk factors. *Stroke*. 2009;40:406–11.
- Inoue T, Shimizu H, Fujimura M, Saito A, Tominaga T. Annual rupture risk of growing unruptured cerebral aneurysms detected by magnetic resonance angiography: clinical article. *J Neurosurg*. 2012;117:20–5.
- Villablanca JP, Duckwiler GR, Jahan R, Tatehima S, Martin NA, Frazee J, Gonzalez NR, Sayre J, Vinuela FV. Natural history of asymptomatic unruptured cerebral aneurysms evaluated at CT angiography: growth and rupture incidence and correlation with epidemiologic risk factors. *Radiology*. 2013;269:258–65.
- Kolega J, Gao L, Mandelbaum M, Mocco J, Siddiqui AH, Natarajan SK, Meng H. Cellular and molecular responses of the basilar terminus to hemodynamics during intracranial aneurysm initiation in a rabbit model. *J Vasc Res*. 2011;48:429–42.
- Kulcsár Z, Ugron A, Marosfo IM, Berentei Z, Paál G, Szikora I. Hemodynamics of cerebral aneurysm initiation: the role of wall shear stress and spatial wall shear stress gradient. *AJNR Am J Neuroradiol*. 2011;32:587–94.
- Szikora I, Paal G, Ugron A, Nasztanovics F, Marosfoi M, Berentei Z, Kulcsar Z, Lee W, Bojtár I, Nyary I. Impact of aneurysmal geometry on intraaneurysmal flow: a computerized flow simulation study. *Neuroradiology*. 2008;50:411–21.
- Cebral JR, Sheridan M, Putman CM. Hemodynamics and bleb formation in intracranial aneurysms. *AJNR Am J Neuroradiol*. 2010;31:304–10.
- Shojima M, Nemoto S, Morita A, Oshima M, Watanabe E, Saito N. Role of shear stress in the blister formation of cerebral aneurysms. *Neurosurgery*. 2010;67:1268–74. discussion 1274–5.
- Tanoue T, Tatehima S, Villablanca JP, Vinuela F, Tanishita K. Wall shear stress distribution inside growing cerebral aneurysm. *AJNR Am J Neuroradiol*. 2011;32:1732–7.
- Sugiyama S, Meng H, Funamoto K, Inoue T, Fujimura M, Nakayama T, Omodaka S, Shimizu H, Takahashi A, Tominaga T. Hemodynamic analysis of growing intracranial aneurysms arising from a posterior inferior cerebellar artery. *World Neurosurg*. 2012;78:462–8.
- Russell JH, Kelson N, Barry M, Percy M, Fletcher DF, Winter CD. Computational fluid dynamic analysis of intracranial aneurysmal bleb formation. *Neurosurgery*. 2013;73:1061–8. discussion 1068–9.
- Sugiyama SI, Endo H, Omodaka S, Endo T, Niizuma K, Rashad S, Nakayama T, Funamoto K, Ohta M, Tominaga T. Daughter sac formation related to blood inflow jet in an intracranial aneurysm. *World Neurosurg*. 2016;96:396–402.
- Boussel L, Rayz V, McCulloch C, Martin A, Acevedo-Bolton G, Lawton M, Higashida R, Smith WS, Young WL, Saloner D. Aneurysm growth occurs at region of low wall shear stress: patient-specific. *Stroke*. 2008;39:2997–3002.
- Brinjikji W, Chung BJ, Jimenez C, Putman C, Kallmes DF, Cebral JR. Hemodynamic differences between unstable and stable unruptured aneurysms independent of size and location: a pilot study. *J Neurointerv Surg*. 2016;9:376–80.
- Sforza DM, Kono K, Tatehima S, Vinuela F, Putman C, Cebral JR. Hemodynamics in growing and stable cerebral aneurysms. *J Neurointerv Surg*. 2016;8:407–12.
- Koffijberg H, Buskens E, Algra A, Wermer MJ, Rinkel GJ. Growth rates of intracranial aneurysms: exploring constancy. *J Neurosurg*. 2008;109:176–85.
- Zhang Y, Mu S, Chen J, Wang S, Li H, Yu H, Jiang F, Yang X. Hemodynamic analysis of intracranial aneurysms with daughter blebs. *Eur Neurol*. 2011;66:359–67.

30. Meng H, Tutino VM, Xiang J, Siddiqui A. High WSS or low WSS? Complex interactions of hemodynamics with intracranial. *AJNR Am J Neuroradiol.* 2014;35:1254–62.
31. Zhu YQ, Li MH, Yan L, Tan HQ, Cheng YS. Arterial wall degeneration plus hemodynamic insult cause arterial wall remodeling. *J Neuropathol Exp Neurol.* 2014;73:808–19.
32. Cebal J, Ollikainen E, Chung BJ, Mut F, Sippola V, Jahromi BR, Tulamo R, Hernesniemi J, Niemelä M, Robertson A, Frösen J. Flow conditions in the intracranial aneurysm lumen are associated with inflammation and degenerative changes of the aneurysm wall. *AJNR Am J Neuroradiol.* 2017;38:119–26.